JOURNAL OF CATALYSIS 133, 486–497 (1992)

Influence of Impregnation Parameters on the Axial Mo/γ-Alumina Profiles Studied Using a Novel Simple Technique

M. A. GOULA, CH. KORDULIS, AND A. LYCOURGHIOTIS[1]

Department of Chemistry, Institute of Chemical Engineering and High-Temperature Processes, University of Patras, GR-26110 Patras, Greece

Received March 14, 1991; revised June 19, 1991

The development of a novel, simple technique allowed us to investigate the influence of various impregnation parameters on the axial Mo profiles achieved on γ-alumina extrudates. The effects of pH, temperature, volume, and concentration of the molybdate solutions, as well as the impregnation time, the rate of drying, the modification of γ-alumina with F^- ions, and the nature and concentration of various competitors, have been systematically studied. It was found that decreases in pH as well as increases in the concentration of the molybdate solutions, of the impregnation temperature, and of the rate of drying cause a progressive transformation of the Mo profile from uniform to eggshell type. Doping of γ-alumina with F^- ions and the use of NH_4F, H_3PO_4, and citric acid as competitors transformed the Mo profiles from eggshell to uniform. The change in volume of the impregnating solution had no effect on the Mo profiles. The effect of the impregnation time was found to be complicated. Increases in the impregnation time, until a critical value sufficient for the complete imbibition of the extrudates, allow for the transfer of great amounts of molybdate to the interior of the extrudates, leading to more uniform profiles. Further increases in the impregnation time caused a considerable increase in the sharpness of the Mo profile. Most of the above observations were explained on the basis of derived equations, adopting a very simple macrodistribution model. Finally, it was demonstrated that small chromatographic columns filled with powder supports may be used to study active ion profiles on catalytic supports.

INTRODUCTION

It is well known that the performance (activity, selectivity, resistance to poisoning) of a supported catalyst can be improved by achieving an appropriate distribution of the active phase within the support grain. Theoretical studies reported in the literature may aid in the achievement of such a distribution in a particular system. The work of Vincent and Merrill (*1*), Komiyama *et al.* (*2*), Schwarz *et al.* (*3–5*), Lee and Aris (*6*), Chou *et al.* (*7*), and Karpe *et al.* (*8, 9*) should be mentioned. A difficulty in this field of industrial catalysis is that the techniques used for determining macrodistribution are in general quite expensive and the instruments necessary are not available in many academic catalysis laboratories.

In most of the studies reported so far, the determination of the macrodistribution of an active phase has been performed using electron probe microanalysis (*2, 10–19*), scanning microscopy (*20*), autoradiography (*4*), light transmission techniques (*2, 11*), and straining methods (*21, 22*). Many studies report Pt-supported γ-alumina catalysts (*4, 13, 14, 16, 21–24*), whereas fewer studies have been performed on Ni (*2, 15, 20*), Cu (*17, 18*), Ba (*20*), Ag (*4*), Cr (*17*), Ph (*12*), and promoted or unpromoted W (*19*) supported γ-alumina catalysts.

Molybdena-supported γ-alumina catalysts are one of the more important classes of solid catalysts not only because they are used industrially (in hydrogenation, dehydrogenation, isomerization, and metathesis) but mainly because they compose the main constituent of the oxidic precursor of [Mo, Co]/γ-Al_2O_3 and [Mo, Ni]/γ-Al_2O_3 catalysts

[1] To whom correspondence should be addressed.

0021-9517/92 $3.00

used in the hydrotreatment of petroleum feedstocks. This is why promoted and unpromoted γ-alumina-supported molybdena catalysts have been the subject of numerous investigations centered on surface characterization and catalytic performance. Studies dealing with the distribution of molybdena within γ-alumina grains are scarce in the literature (*25, 26*). The first macrodistribution study on $MoO_3/\gamma\text{-}Al_2O_3$ catalysts was reported by Srinivasan *et al.* (*25*), who showed that conventional impregnation of alumina pellets with aqueous ammonium paramolybdate (AHM), followed by drying and calcining, can lead to an eggshell macrodistribution. Moreover, movement of the shell boundaries toward the pellet center has been observed on sintering at 750°C. A fine study on this subject was communicated some years ago by Fierro *et al.* (*26*). The main goal was to obtain Mo and Co concentration profiles within γ-alumina pellets by controlling pH, impregnation time, and solute concentration. Two extreme macrodistributions of Mo have been obtained: eggshell and uniform. Low pH (2.8), small impregnation time (1 h), and high solute concentration (0.055 *M* AHM) favor the former. In contrast, alkaline solutions (pH 10.8), high impregnation time (72 h), and low solute concentration (0.018 *M* AHM) are required to obtain uniform distribution. On the so-achieved $MoO_3/\gamma\text{-}Al_2O_3$ catalysts with uniform profile, cobalt has been deposited in eggshell distribution. It is obvious that in this case the critical ratio Co/[Co + Mo] decreases from the outer surface to the axis of the extrudate. An increasing value for the Co/[Co + Mo] ratio from the periphery to the axis has been obtained by depositing cobalt on $MoO_3/\gamma\text{-}Al_2O_3$ catalysts with eggshell distribution. Finally, a constant value for the atomic ratio Co/[Co + Mo] has been obtained by capillary coimpregnation of molybdenum and cobalt.

In the frame of a research program recently undertaken in our laboratory the following items were addressed: (i) We attempted to develop a very simple technique allowing the determination of axial macrodistribution in extrudates. This technique should be quantitative and suitable for all active elements determined by usual analytical techniques. (ii) Using the technique mentioned above, we wanted to be able to study systematically the influence of the various impregnation parameters on Mo profile within the γ-alumina extrudates. (iii) On the basis of findings of the above mentioned study, we tried to obtain all profiles (eggshell, egg white, egg yolk, and uniform) both axially and radially and to characterize the active phase for the radial profiles obtained. This characterization is expected to help us to examine whether, for a constant amount of supported molybdenum, the type of profile obtained and the volume of the support occupied by the active phase are related to its structure and texture (dispersion, symmetry, interaction with support, etc.). This information is of paramount importance for the appropriate design of preparation procedures of catalysts, in which the "microscopic characteristics" of the active phase, which are related to the number and quality of the active centers, should be taken into account. (iv) We attempted to relate the catalytic activity and selectivity with the profile obtained using a simple probe reaction. (v) We repeated points (ii)–(iv) for materials promoted with Co and Ni. In the present paper we deal with points (i) and (ii).

EXPERIMENTAL

Substances–Solutions

γ-Alumina pellets of 7-mm length and 3.2-mm diameter were used in the present study. The composition of the pellets was 97% $\gamma\text{-}Al_2O_3$, 0.05% SiO_2, and 0.7% Na_2O. The specific surface area (SSA) and the average pore diameter were respectively 120 $m^2 \cdot g^{-1}$ and 110 Å (monomodal). The water pore volume was 0.35 $cm^3 \cdot g^{-1}$.

Ammonium heptamolybdate, $(NH_4)_6Mo_7O_{24} \cdot 4H_2O$, obtained from Riedel de Haen (99%), was used for the preparation of the molybdate aqueous solutions. The pH of these solutions was adjusted to values lower

or higher than the point of zero charge of γ-Al_2O_3, equal to 5.3, by adding HNO_3 or NH_4OH, as needed.

Ammonium nitrate, obtained from Riedel de Haen (99%), was used to adjust the ionic strength of the molybdate solutions.

The F^--doped γ-alumina samples were prepared by impregnating the extrudates with aqueous solutions of ammonium fluoride, NH_4F (Carlo Erba R.P.). Following impregnation, the specimens were dried at 120°C for 2 h and then air-calcined at 520°C for 15 h.

Aqueous solutions of phosphoric acid, H_3PO_4 (Sigma), ammonium fluoride, NH_4F (Carlo Erba R.P.), and citric acid (Sigma) were used as competitors.

Procedure for the Determination of the Axial Distribution

The technique developed in the present work for determining the axial or lengthwise distribution involves three steps: (i) the "preparation" of the samples, (ii) the impregnation procedure, and (iii) the determination of the concentration gradient extending halfway from the extrudate to the ends.

The lengths of a large number of extrudates were accurately measured and 20 pellets with lengths exactly equal to 7 mm were selected for each experiment. Each pellet was next covered with a flexible plastic tube having diameter a little smaller than that of the extrudate. Imbibition experiments, described in the next paragraph, with colored water showed that this technique ensured good fitting and prevented the liquid imbibition from the lateral surface of the cylinder, allowing the "production" of a lengthwise distribution of the deposited molybdenum.

Two grams of the extrudates was immersed over time in 20 cm^3 of impregnation (molybdate or molybdate competitor) solution of a given concentration, at constant pH and temperature. Next, the impregnated extrudates were dried at 120°C for 2 h.

The dried extrudates were divided into 10 slices of equal thickness (0.7 mm) using a cutting tool made in the laboratory (Fig. 1A) and the plastic covers were removed. The slices located at the same distance from the center of the cylinders were then separated and weighed. Molybdenum was extracted by treating each sample (~0.2 g) with 2 cm^3 of an ammonia solution (0.1 N, pH 10) for 17 h. Following filtration the extracted Mo was determined spectrophotometrically at 490 nm (Varian Carry 219) (*27*). In all cases the total molybdenum extracted was almost equal to that adsorbed during impregnation.

By using this technique, it was possible to draw "N vs X" curves, i.e., of the Mo loading (μmol · m^{-2}), N, determined in the slice at distance X from an edge of the extrudates. To compare the results obtained from this technique with those obtained with electron probe microscopic analysis (EPMA) it was necessary to calculate the atomic ratio Mo/Al for each value of $(L - l)/L$ (see Fig. 1B). The calculation was done by using the expression

$$\frac{\text{Mo}}{\text{Al}} = \frac{N \times \text{SSA} \times W \times 51 \times 10^{-6}}{W - N \times \text{SSA} \times W \times 1235.86 \times 10^{-6}}$$

where W is the weight of each slice (g), and the ratio Mo/Al at a given $(R - r)/R$ value (see Fig. 1B) was determined for pellets impregnated, without plastic cover, using a Jeol temsam 10 cx electron microscope equipped with a Kevex energy dispersive analyzer. It was thus possible to compare the lengthwise distribution effected by our technique with the radial distribution obtained using EPMA.

Observation of Liquid Imbibition from the Pellets

The observation of liquid imbibition into a pellet was performed by optical microscopy. Covered or uncovered pellets were immersed in colored water for periods ranging from 3 s to 6 min and the movement of the liquid front was observed using an optical microscope. It was thus possible to determine the time required for axial or radial

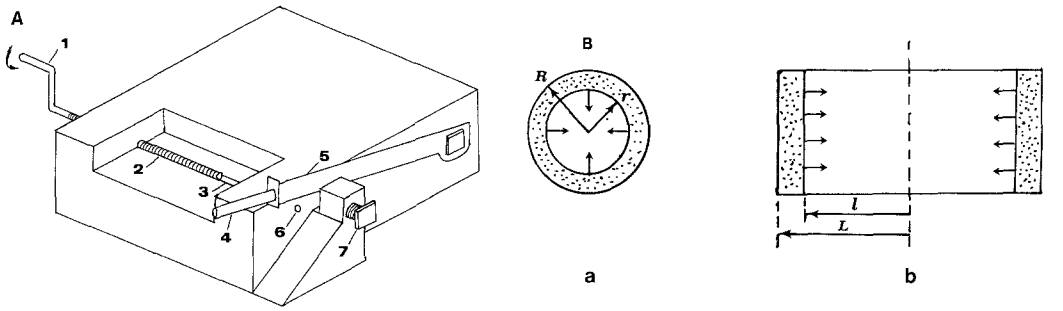

FIG. 1. (A) Schematic representation of the laboratory-made cutting tool used in the present work. 1, Revolving handle. 2, Long screw thread (screw pitch = 0.7 mm). 3, Long screw and extrudate ditch guide. 4, Knife handle. 5, Knife. 6, Extrudate exit hole. 7, Knife adjusting screw. (B) Schematic representation of (a) radial and (b) axial imbibition of an alumina extrudate.

liquid imbibition of an extrudate to be completed.

RESULTS AND DISCUSSION

Theoretical Remarks

The study of the influence of the various impregnation parameters on the Mo profile becomes clearer if it is based on a theoretical model that may reveal the physicochemical parameters on which the macrodistribution features depend. The "simplified version" of the Lee and Aris model (*6*) was used in the present work. This model developed for spherical particles may be easily transformed to describe axial and radial macrodistribution in extrudates. Assuming that the catalyst support is a homogeneous porous cylinder, the support surface is wetted by an incompressible aqueous solution, the total amount of impregnating solution is greater than the total void volume of the support, the pores of the support are large enough so that no physical exclusion of solute occurs, the immobilization of solute on the surface is an isothermal, reversible Langmuir adsorption whose characteristics do not change with the variation of solute concentration during the impregnation process, the resistance to mass transfer of solute at the liquid–pore wall interface is negligibly small, and there is no surface diffusion of the adsorbed solute. Following a procedure similar to that of Aris and Lee Eqs. (1) and (2), suitable for describing axial and radial macrodistributions in extrudates, respectively, may be easily obtained.

$$\Gamma_a = \frac{\tau}{1 + \alpha n_s K/(1 + KC_0)} \quad \text{(axial)} \quad (1)$$

$$\Gamma_r = 1 - \left[1 - \frac{\tau}{1 + \alpha n_s K/(1 + KC_0)}\right]^{(1/2)} \quad \text{(radial)}, \quad (2)$$

where τ, α, n_s, K, and C_0 represent, respectively, the reduced impregnation time defined as t/t_L (t_L/min: time required for the liquid imbibition to be accomplished), the ratio of the specific surface area to the pore volume (m^{-1}), the saturation surface concentration of the adsorption sites (μmol m^{-2}), the adsorption constant, and the initial concentration of the impregnating solution. Γ_a and Γ_r are defined, respectively, by $L - l/L$ and $R - r/R$ (Fig. 1B). It is obvious that $\Gamma_{a,r}$ may be used to describe the type of macrodistribution: low (high) values of $\Gamma_{a,r}$ imply eggshell macrodistributions. A relationship between Γ_a and Γ_r may be easily obtained by combining Eqs. (1) and (2).

$$\Gamma_r = 1 - [1 - \Gamma_a]^{1/2} \quad (3)$$

Comparison of Axial and Radial Profiles

In Fig. 2 a typical eggshell profile obtained at relatively low pH and over a period of

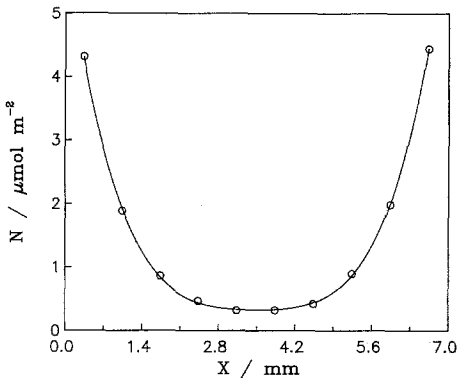

FIG. 2. A typical eggshell Mo profile achieved using the technique described under Experimental (pH 4.5, $\tau = 10$, $T = 25°C$, $C_0 = 0.7\ M$).

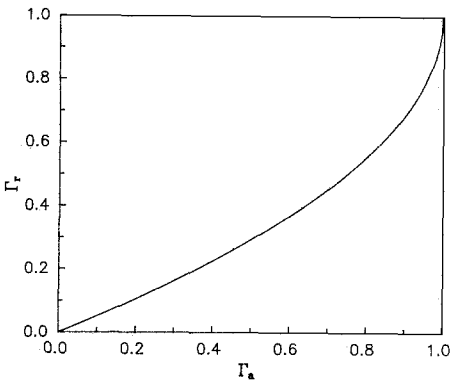

FIG. 3. Plot of Eq. (3).

1 h may be seen. It should be noted that the concentration profile is quite symmetrical, suggesting that the technique developed is accurate. Moreover, as already mentioned in the introduction, an eggshell profile was anticipated for relatively low pH and short impregnation time.

Apparently, as far as the catalyst preparation is concerned, the prediction of a radial profile for a given set of preparative parameters is much more interesting compared with the prediction of the axial profile. It is therefore plausible to question whether radial profiles may be predicted provided that axial profiles are known. This may, in principle, be achieved on the basis of Eq. (3). Moreover, the graphical representation of Eq. (3), Fig. 3, shows that similar, though not identical, axial and radial profiles should be obtained under identical preparative conditions. To check this point it is necessary to compare our results with the results obtained by the classical EPMA technique under identical conditions, namely, the same pH, temperature, solute concentration, V_{solute}/V_p ratio (V_p, pore volume), and dimensionless impregnation time. In Fig. 4 typical comparative profiles are presented. Taking into account the precision of EPMA, the agreement achieved is satisfactory. This demonstrates that the technique proposed in the present work may be used not only for studying the influence of the various impregnation parameters on the axial profiles but also for determining the precise values of the impregnation parameters needed for the radial profile desired.

Influence of the Various Impregnation Parameters on the Mo Profile

Next, we examined the influence of the various impregnation parameters on the Mo profile. To estimate the sharpness of the N vs X profiles (see Fig. 2) we used the parameter, s, defined as $(dN/dX)_{x=0}/\Sigma Ni$. It is obvious that as the profile becomes more uniform the value of s decreases and equals

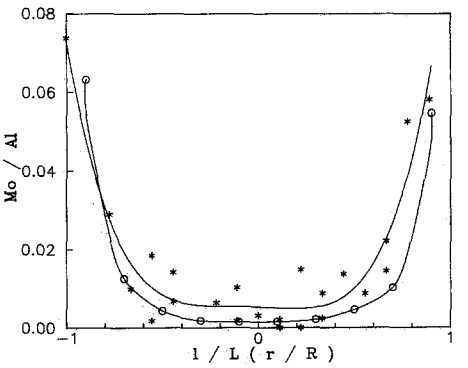

FIG. 4. Comparison of axial (○) and radial (*) Mo profiles obtained under the same experimental conditions using the present technique and EPMA, respectively (pH 4.5, $\tau = 1$, $T = 25°C$, $C_0 = 0.7\ M$).

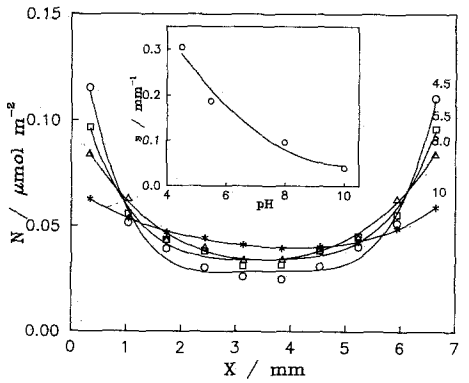

FIG. 5. Mo profiles obtained at various pH values shown on the curves (τ = 1, T = 25°C, C_0 = 0.02 M).

zero in the case of a completely uniform distribution.

Influence of pH. The Mo profiles obtained over a pH range between pH 4 and 10 are shown in Fig. 5, in which a transformation of the profile from eggshell into uniform as pH increases should be noted. This result, which is in agreement with the literature (*26*), may be interpreted as follows: It is known that the charging mechanism of the surface of γ-alumina may be described using the relevant protonation/deprotonation equilibria (*28*),

$$\mathrm{AlOH_2^+} \underset{K_2}{\overset{K_1}{\leftrightarrows}} \mathrm{AlOH} + \mathrm{H_s^+}$$

$$\mathrm{AlOH} \leftrightarrows \mathrm{AlO^-} + \mathrm{Hs}$$

$$\mathrm{H_s} \rightleftarrows \mathrm{H_b^+}$$

where by AlOH, $AlOH_2^+$, and AlO^- we denote respectively the neutral, protonated, and deprotonated surface hydroxyls and by H_s^+ and H_b^+ the surface and bulk-solution hydrogen ions, respectively. From the above equilibria, it may be seen that an increase in the pH would decrease the concentration of the protonated surface hydroxyls. This fact has indeed been experimentally confirmed (*29–31*). Moreover, recent studies (*32–34*) have shown that the molybdates are adsorbed on the inner Helmholtz plane of the double layer around the powder support particles suspended in aqueous molybdate solutions and that the density of the adsorption sites is an increasing function of the concentration of the $AlOH_2^+$ groups, considered to be responsible for the creation of the adsorption sites. It may, therefore, be anticipated that at higher pH there will be less adsorption sites, n_s. This fact is demonstrated in Table 1, in which the n_s values, determined by interpolation using results from Ref. (*33*), for pH values corresponding to those at which our profiles were obtained, are shown. Finally, according to Eq. (1) a decrease in n_s, as pH increases, should cause an increase in the value of Γ_a and this would therefore lead to a progressive transformation of the Mo profile from eggshell to uniform, which is in full agreement with our experimental results.

The above considerations are valid provided that the other parameters involved in Eq. (1) are not changed with pH. Although this is obvious for α and C_0 the adsorption constant has been found to vary randomly with pH (*33*). Moreover, as K appears both in the numerator and in the denominator, its variation is not expected to affect considerably the value of Γ_a.

Influence of temperature on the impregnating solution. It is shown in Fig. 5 that an eggshell profile with a high s value may be obtained at relatively low pH values (pH 4.5). The question raised at this point is whether it is possible to further increase the sharpness of the distribution by depositing larger amounts of molybdate species at the

TABLE 1

n_s Values Calculated[a] at pH Values at which Mo Profiles Have Been Obtained

pH	n_s/μmol · m^{-2}
4.5	9.9
5.5	5.2
8.0	0.2
10.0	0.1

[a] See text; T = 25°C.

TABLE 2

n_s Values Calculated[a] at Various Temperatures at which Mo Profiles Were Obtained

T(°C)	n_s/μmol · m^{-2}
25	9.9
35	11.7
45	13.7
55	17.7

[a] See text; pH 4.5.

two ends of the extrudates. Further pH decrease was not considered the appropriate way, because the dissolution of the γ-alumina would increase considerably whereas the increasing polymerization of the Mo(vi) species, occurring at low pH values, has been related with the decrease of the mean adsorption constant. It is mainly for these reasons that the uptake of Mo(vi) species on γ-alumina powder was found to decrease as the pH decreased from 4.5 to 3.0, suggesting a decrease in the n_s value. In fact, for this pH change n_s was found to decrease from 9.9 to 7.47 μmol · m^{-2} (*33*).

The surface protonation/deprotonation charging mechanism implies that the concentration of $AlOH_2^+$ groups and therefore of n_s may be increased by decreasing the values of the acidity constants K_1 and K_2, which are in general temperature dependent. Earlier work (*30*) has shown that when the solution temperature is increased, the values of K_1 and K_2 decreased, consequently increasing the concentration of the $AlOH_2^+$ groups at constant pH. Recently, additional studies have shown that the increase in the concentration of the $AlOH_2^+$ groups resulted in increased n_s values (*33*). In Table 2 the values of n_s obtained over a temperature range between 25 and 55°C, over which Mo profiles were obtained, may be seen. The values in Table 2 have been taken from the results of Ref. (*33*). It may be seen that upon an increase in the temperature of impregnating solution the value of n_s increased. Consequently, a decrease in the value of Γ_a (see Eq. (1)) and therefore an increase in the sharpness were anticipated. Our experimental results, as seen in Fig. 6, are in excellent agreement with the predicted values. As may be seen, upon an increase in the impregnating solution temperature at pH 4.5 from 25 to 55°C, the sharpness increased from 0.52 to 2.55.

Modification of the Mo profile by doping the γ-alumina extrudates with varying amounts of F^- ions. It has been recently reported (*29*) that doping of γ-alumina with varying amounts of fluoride ions caused a decrease in the point of zero charge of this support and thus a decrease in the concentration of the positive surface groups, $AlOH_2^+$, considered responsible for the creation of the adsorption sites for the molybdates. It may, therefore, be anticipated that the Mo profile obtained on extrudates doped with fluoride ions would have a lower s value than the undoped extrudates. As seen in Fig. 7, this prediction was confirmed, indicating that the modification of the γ-alumina extrudates with F^- ions may be used to obtain more uniform macrodistributions.

Influence of the impregnation time. Using the technique described under Experimental, we have found that the time required for the axial liquid imbibition, t_L, is 6 min. In Fig. 8 the Mo profiles obtained at various values of τ and at constant pH, T, and C_0 may be seen. It may be noted that increase

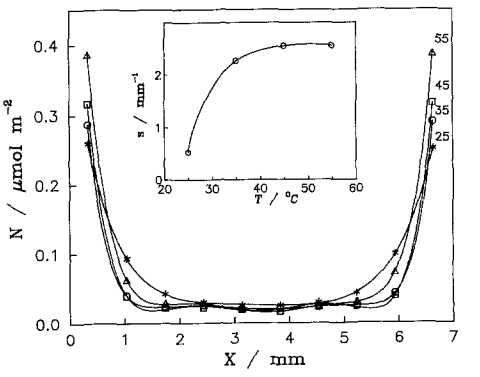

FIG. 6. Mo profiles at various temperatures, shown on the curves (τ = 10, pH 4.5, C_0 = 0.02 M).

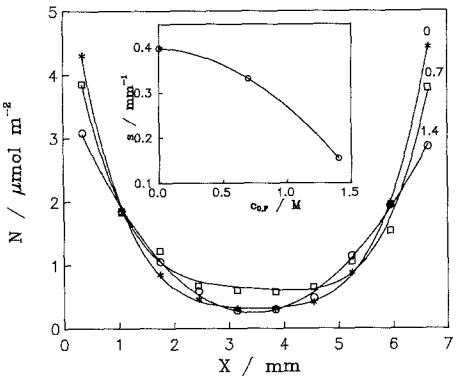

FIG. 7. Mo profiles at γ-alumina extrudates doped with various amounts of F^- anions. The values of F^- content ($C_{0,F}$) are indicated (τ = 10, pH 4.5, T = 25°C, C_0 = 0.7 M) on the corresponding curves.

in the τ value, from 0.1 to 1, resulted in a decrease in the sharpness from 0.45 to 0.30. In this τ range the solute transfer takes place mainly through capillary forces, which is a fundamental assumption for the derivation of Eq. (1). In fact, Eq. (1) predicts an increase in the value of Γ_a and thus a decrease in the value of s as τ increases.

A further increase in the value of τ from 1 to 30 caused a considerable increase in the sharpness, favoring the deposition at the ends of the extrudates. This may be interpreted by taking into account that in this τ range the solute transfer from the ends to the interior of the already soaked extrudates takes place by diffusion, a rather slow process in comparison with the adsorption of the molybdates on the γ-alumina surface. The increasing trend in the s value with τ should be limited because past a time period, depending mainly on the solution pH, the adsorption of the molybdates on the γ-alumina surface reaches equilibrium. For τ values exceeding the "equilibrium" time, therefore, the trend is expected to reverse.

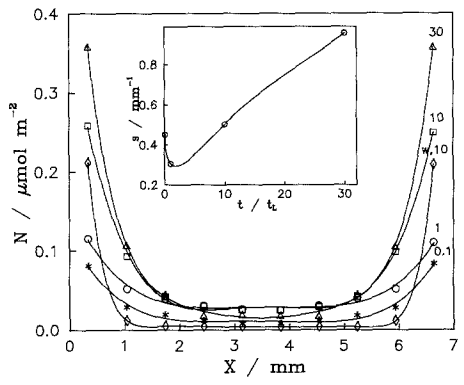

FIG. 8. Mo profiles at various impregnation times. The values of τ are indicated (pH 4.5, T = 25°C, C_0 = 0.02 M) on the corresponding curves. The curve represents Mo profile achieved on extrudates preimpregnated with pure solvent (s = 3.8613).

The above findings suggest that an egg-shell distribution with very high s value should be obtained when diffusion is the sole mechanism for the solute transfer. This can be easily achieved by impregnating the extrudates in the pure solvent for $\tau > 1$ and then impregnating the soaked extrudates in molybdate solutions for $1 < \tau <$ equilibrium time. In Fig. 8, experimental confirmation of the aforementioned predictions (curve w) is shown.

Effect of the rate of drying on the Mo profile. The above considerations showed that the lower limit in the s variation with time was obtained for τ = 1. Beyond this point, s increased with time because the rate of adsorption on the outer parts of the extrudates is higher than the rate of diffusion of the molybdates into the internal parts of the extrudates. The additional adsorption of the molybdates, therefore, on the outer layers of the extrudates should be avoided when a uniform macrodistribution is sought. This may be obtained by separating the bulk solution from the extrudates at τ = 1 and allowing the extrudates to dry very slowly at room temperature for 24 h. The low rate of drying is expected to allow the transfer of the solute into the internal parts of the extrudates and the achievement of a uniform profile. This was confirmed experimentally, as seen in Fig. 9.

Influence of the molybdate concentration on the Mo profile. The Mo profiles obtained over a range of molybdate concentrations and constant temperature, impregnation

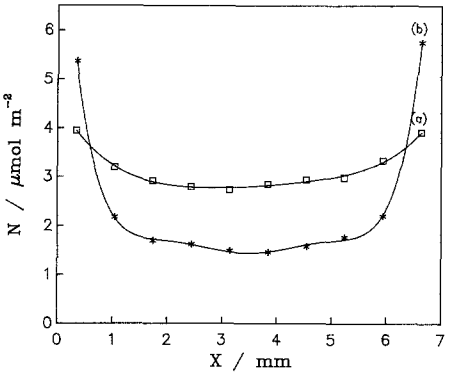

FIG. 9. Mo profiles obtained at two rates of drying. (a) Slow drying at room temperatures for 24 h (s = 0.06718); (b) fast drying at 120°C for 24 h (s = 0.6965) (pH 10, T = 25°C, τ = 1, C_0 = 1 M).

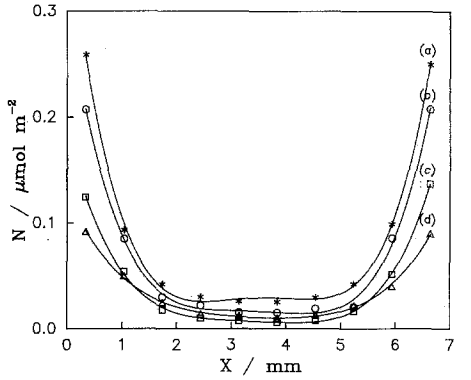

FIG. 11. Mo profile in the presence of various competitors. (a) Without competitors; (b) NH_4F; (c) H_3PO_4; (d) citric acid (pH 4.5, τ = 10, $C_{0,1}$ = 0.02 M, $C_{0,2}$ = 0.7 M, T = 25°C).

time, and initial pH are shown in Fig. 10. It may be observed that an increase in the concentration of the molybdates resulted in an increase of the s value contrary to the prediction of Eq. (1). The discrepancy between prediction and experimental results may be explained as follows: It has been recently observed (*32, 33*) that the adsorption of molybdate on γ-alumina powder is accompanied by an increase in the pH of the impregnating solution. The difference $pH_f - pH_{in}$ (pH_{in}, pH_f represent respectively the pH before and after adsorption) decreases progressively with C_0. Taking into account that in our experiments pH_{in} is constant, it was expected that the pH_f would decrease with the C_0 value. As already mentioned, however, a decrease in pH would increase the n_s value, which in turn would decrease (increase) $\Gamma(s)$. Our results indicate that the primary effect of C_0 on Γ or s is weaker than the secondary effect of n_s on these parameters.

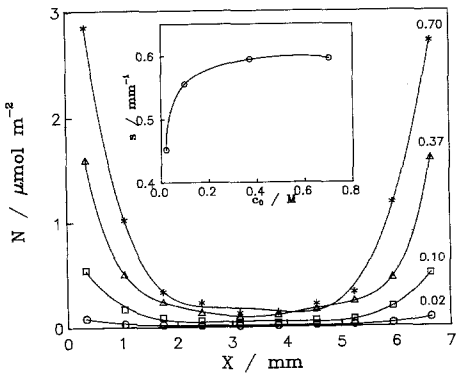

FIG. 10. Mo profiles obtained at various concentrations of the molybdate solution. The values of C_0 are indicated (pH 4.5, T = 25°C, τ = .1).

Effect of the impregnating solution volume on the Mo profile. In agreement with the theoretical predictions (see Eq. (1)) it was found that a change in the V_s/V_p ratio (V_s, V_p represent respectively the volume of the impregnating solution and the water pore volume of γ-alumina) did not have any considerable effect on the Mo profiles.

Use of competitors for regulating the Mo profile. The use of competitors for regulating the active ion profiles is well known (*5, 6, 10, 11, 13, 35, 36*). The anions of the competitors compete with the anions to be supported for the same adsorption sites, causing a decrease in the loading and rendering the profile more uniform. Figure 11 illustrates the effects of various competitors on the Mo profile. As may be seen, the most considerable decrease was found for citric acid. Moreover, it was observed in all cases that the sharpness decreased and the profile became more uniform as the ratio [$C_{competitor}$/

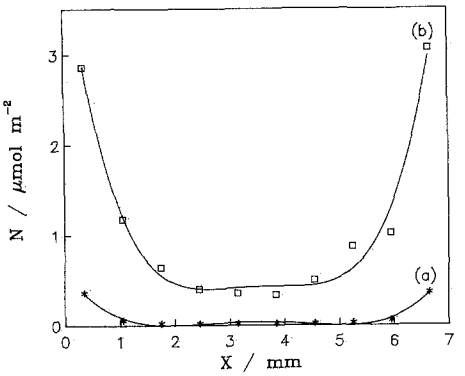

FIG. 12. The effect of the $C_{0,1}/C_{0,2}$ on the Mo profiles in the presence of H_3PO_4 (a) $C_{0,1}/C_{0,2}$ = 0.02/0.7; (b) $C_{0,1}/C_{0,2}$ = 0.35/0.7 (pH 4.5, τ = 30, T = 25°C).

$C_{molybdates}$] increased. A typical example is shown in Fig. 12. The second observation may be explained on the basis of the equation

$$\Gamma_a = \tau/\left(1 + \frac{\alpha n_s K_1^*}{1 + K_1^* C_{0,1} + K_2^* C_{0,2}}\right), \quad (4)$$

where K_1^*, $C_{0,1}$, K_2^*, and $C_{0,2}$ represent the adsorption constant and the concentration of the molybdates and those of the anions of the competitor, respectively. The first observation may also be explained by assuming that the value of K_2^* for the citric acid anions is greater than the corresponding values for the F^- and PO_4^{3-} anions.

It should be noted that Eq. (4) may be easily derived for axial distribution in extrudates, adopting the simplified version of the Lee and Aris model (*6*), the assumption mentioned under Theoretical Remarks, and assuming that the anions of the competitor compete with the molybdates for the same adsorption sites.

Simulation of an Extrudate with a Small Chromatographic Column

The study of the influence of the various impregnation parameters on the Mo profiles and the simplified model adopted are based on the assumption that the main fundamental processes involved are the adsorption and desorption of the molybdates on/from the γ-alumina surface as well as its axial transfer to the center of the extrudate. It is, however, well known that the same processes are involved during separations in the liquid–solid chromatography. It is therefore interesting to examine whether it is possible to simulate an extrudate with a small chromatographic column. We have thus filled a cylindrical plastic tube (l = 5.6 mm, d = 1.5 mm) with γ-alumina powder prepared by crushing the extrudates. After a compact packing and closing of the ends of the tube with glass wool, the procedure described under Experimental for determining the axial distribution (except for the slicing part) was followed and the Mo distribution throughout the tube was determined. As seen in Fig. 13, there was no considerable difference between the Mo profile obtained using extrudates and that obtained following the above procedure.

Our experimental approach therefore demonstrated that small chromatographic columns filled with powder supports may be used to study active ion profiles on catalytic supports. Our simple experimental technique may be used when a large number of experimental points are required for the construction of the curves describing profiles and it should be considered as complementary to the extrudate slicing technique presented in this work.

Comparison of the Method with Other Important Methods Used for Measuring Concentration Profiles

It has been proved that the method presented here can be used to determine various impregnation parameters in order for a desired radial profile to be achieved. This method is most suitable for studying axial profiles. Other techniques (e.g., EPMA and light transmission technique) could be used and are compared to our procedure in Table 3. Inspection of this table illustrates that the method developed here has some advan-

TABLE 3

Comparison of Different Techniques Used (or that Could Be Used) to Study Axial Profiles in Extrudates

Characteristic	Our method	EPMA[a]	Light transmission
Cost	Low	High	Low
Accuracy	High	Medium	Medium
Simplicity	Very simple	Quite complicated (special holders and cutting apparatus required)	Simple[2]
Applicability	Applicable for all active ions	Applicable for all active ions	Could only be applied in colored samples[c]
Spatial resolution	Low	High	Medium

[a] EPMA has so far not been used to study axial profiles.

[b] Requires photographic negatives. These should be analyzed using a scanning microdensitometer (Refs. (*4*, *5*)).

[c] When the active ions should be colored, usually by reduction, the intensity of the color is not necessarily related directly with the amount of active ion deposited because it also depends on the extent of reduction, which in turn is affected by the symmetry and dispersity of the active species.

tages over other techniques of significance, such as low cost, high accuracy and simplicity, as well as wide applicability.

CONCLUSIONS

From the present work the following conclusions may be drawn:

(i) The technique described here can be used to study axial and to predict radial macrodistributions in extrudates.

(ii) A decrease in pH as well as increases in the concentrations of the molybdate solutions, of the impregnation temperature, and the rate of drying caused a progressive transformation of the Mo profile from uniform to eggshell. The opposite trend was obtained by doping γ-alumina extrudates with F^- ions or by using NH_4F, H_3PO_4, and citric acid as competitors, whereas no appreciable effect on the Mo profile was obtained by changing the volume of the impregnating solution. An increase in the impregnation time to a value corresponding to the completion time favored the progressive transformation of the Mo profile from eggshell to uniform. The opposite effect was obtained by further increasing the impregnation time.

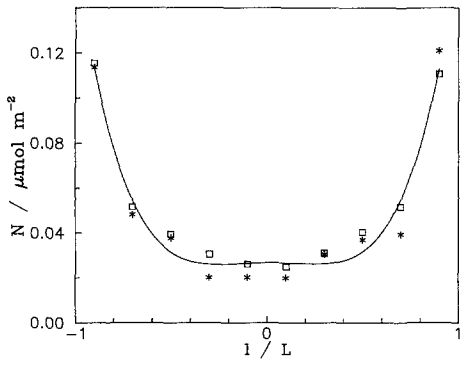

FIG. 13. Mo profiles obtained using γ-alumina extrudates and a small chromatographic column (pH 4.5, $\tau = 1$, $T = 25°C$, $C_0 = 0.02\ M$).

(iii) Small chromatographic columns filled with powder supports may be used to study axial profiles on catalytic supports when a relatively large number of experimental points is required.

The present study showed that only two types (eggshell and uniform) of Mo profiles may be obtained by changing the values of the parameters mentioned above. Alternative methods should therefore be developed for obtaining, both axially and radially, egg-white and egg-yolk Mo profiles. The preparation and the detailed characterization of

Mo catalysts with all types of macrodistribution are the subjects of the second paper in this series.

REFERENCES

1. Vincent, R. C., and Merrill, R. P., *J. Catal.* **35,** 206 (1974).
2. Komiyama, M., Merrill, R. P., and Harnsberger, H. F., *J. Catal.* **63,** 35 (1980).
3. Kulkarni, S. S., Mauze, G. R., and Schwarz, J. A., *J. Catal.* **69,** 445 (1981).
4. Heise, M. S., and Schwarz, J. A., *J. Colloid Interface Sci.* **107,** 237 (1985).
5. Schwarz, J. A., and Heise, M. S., *J. Colloid Interface Sci.* **135,** 461 (1990).
6. Lee, S. Y., and Aris, R., *Catal. Rev. Sci. Eng.,* **27**(2), 207 (1985).
7. Chou, P., Petersen, E. E., and Radke, C. J., *J. Catal.* **117,** 52 (1980).
8. Karpe, P., and Ruckenstein, E., *Colloid Polym. Sci.* **267,** 145 (1989).
9. Ruckenstein, E., and Karpe, R., *Langmuir* **5,** 1393 (1989).
10. Becker, E. R., and Nuttall, T. A., *Prep. Catal. 2,* 159 (1979).
11. Hegedus, L. L., Chou, T. S., Summers, J. C., and Potter, N. M., *Prep. Catal. 2,* 171 (1979).
12. Van den Berg, G. H., and Rijnten, H. Th., *Prep. Catal. 2,* 265 (1979).
13. Shyr, V. S., and Ernst, W. R., *J. Catal.* **63,** 425 (1980).
14. Fujiyama, T., Otsuka, M., Tsuiki, H., and Veno, A., *J. Catal.* **104,** 323 (1987).
15. Roth, J. F., and Reichard, T. E., *J. Res. Inst. Catal.* **20,** 84 (1972).
16. Chen, H.-C., and Anderson, R. B., *J. Catal.* **43,** 200 (1976).
17. Ott, R. J., and Baiker, A., *Prep. Catal. 2,* 685 (1982).
18. Maitra, A. M., Cant, N. W., and Trimm, D. L., *Appl. Catal.* **27,** 9 (1986).
19. Melo, F., Cervello, J., and Hermana, E., *Chem. Eng. Sci.* **35,** 2175 (1980).
20. Harriott, P., *J. Catal.* **14,** 43 (1969).
21. Maatman, R. W., and Prater, *Ind. Eng. Chem.* **49,** 253 (1957).
22. Maatman, R. W., *Ind. Eng. Chem.* **51,** 913 (1959).
23. Michalko, E., U.S. Patent 3,259,589 (1966).
24. Summers, J. C., and Ausen, S. A., *J. Catal.* **52,** 445 (1978).
25. Srinivasan, R., Liu, H.-C., and Weller, S. W., *J. Catal.* **57,** 87 (1979).
26. Fierro, J. L. G., Grange, P., and Delmon, B., *Prep. Catal. 3,* 591 (1982).
27. Snell, F. D., "Photometric and Fluorometric Methods of Analysis of Metals," Vol. 2, p. 1296. Wiley, New York, 1978.
28. Vordonis, L., Koutsoukos, P. G., and Lycourghiotis, A., *J. Catal.* **98,** 296 (1986).
29. Vordonis, L., Koutsoukos, P. G., and Lycourghiotis, A., *J. Catal.* **101,** 186 (1986).
30. Akratopulu, K., Vordonis, L., and Lycourghiotis, A., *J. Chem. Soc. Faraday Trans. 1* **82,** 3697 (1986).
31. Vordonis, L., Koutsoukos, P. G., and Lycourghiotis, A., *J. Chem. Soc. Chem. Commun.,* 1309 (1984).
32. Spanos, N., Vordonis, L., Kordulis, Ch., and Lycourghiotis, A., *J. Catal.* **124,** 301 (1990).
33. Spanos, N., Vordonis, L., Kordulis, Ch., Koutsoukos, P. G., and Lycourghiotis, A., *J. Catal.* **124,** 315 (1990).
34. Vordonis, L., Koutsoukos, P. G., and Lycourghiotis, A., *Colloids Surf.* **50,** 353 (1990).
35. Wang, J., Zhang, J., and Pang, L., *Prep. Catal. 3,* 57 (1982).
36. Castro, A. A., Scelza, O. A., Benvenuto, E. R., Baronetti, G. T., De Mignel, S. R., and Parera, J. M., *Prep. Catal. 3,* 47 (1982).